International Journal of Computer Information Systems and Industrial Management Applications
ISSN 2150-7988 Volume 18(13s) 2026 pp. 995-1011
https://doi.org/10.70917/ijcisim-2026-4144
Article

Design and Experimental Validation of a Bidirectional DC–DC Converter for Charging a Lead-Acid Battery from a PV Panel

Ahmed Khalaf Hammad[1], Arkan Ahmed Hussein[2,*]

[1] Department of Electrical Engineering, University of Tikrit, Tikrit, Iraq
[2] Department of electrical engineering, University of Tikrit, Tikrit, Iraq **Corresponding Author:**
Arkan Ahmed Hussein (E-mail: aalganabe@tu.edu.iq)

Abstract: Reliable battery charging remains a major challenge in standalone photovoltaic (PV) systems operating under continuously varying environmental conditions. This paper presents the experimental validation of an experimentally optimized priority-based finite-state machine (EO-PFSM) controller for a non-isolated bidirectional buck–boost DC–DC converter used to charge a 48 V lead-acid battery from a 340 W PV module. Unlike conventional charging techniques that continuously adjust the duty cycle through optimization-based algorithms, the proposed controller employs predefined PWM commands associated with discrete charging states, thereby reducing computational complexity while maintaining reliable charging performance. The controller was implemented using an Arduino Mega 2560 and experimentally evaluated under real outdoor operating conditions. A total of 1,039 operating samples were recorded during approximately two hours of testing. After excluding the startup transient interval, 1,012 valid steady-state samples were used for electrical and statistical analyses. The experimental results demonstrated stable transitions between the BOOST, BULK, and FLOAT charging stages while achieving an average converter efficiency of 94.06%. Furthermore, an independent logic-based load management strategy was successfully integrated without affecting the charging process. The obtained results demonstrate that the proposed EO-PFSM controller provides an effective balance between implementation simplicity, computational efficiency, charging reliability, and practical applicability for standalone photovoltaic battery charging systems.
Keywords: Bidirectional DC–DC converter, finite state machine, lead-acid battery charging, non-isolated buck-boost, photovoltaic energy

1. INTRODUCTION

The increasing deployment of standalone photovoltaic (PV) systems has accelerated the demand for efficient and reliable battery charging solutions in remote residential, agricultural, and telecommunication applications where grid access is unavailable or limited [1]–[3]. In these systems, battery energy storage plays a vital role in maintaining uninterrupted power supply during periods of low solar irradiance and nighttime operation, making the battery charging controller a key factor affecting system efficiency, reliability, and battery lifetime [4],[10].A DC–DC converter is commonly employed to regulate the power transfer between the PV source and the battery bank. Among the available converter topologies, the non-isolated bidirectional buck–boost converter has attracted considerable attention because of its simple structure, high efficiency, reduced component count, and capability of supporting bidirectional power transfer [2],[3],[11],[13]. These characteristics make it well suited for standalone renewable-energy systems incorporating battery energy storage.Conventional battery charging strategies generally combine constant-current/constant-voltage (CC–CV) regulation with maximum power point tracking (MPPT) algorithms such as Perturb and Observe (P&O) and Incremental Conductance (INC). Although these approaches provide satisfactory charging performance, they usually rely on continuous duty-cycle optimization, resulting in increased computational complexity and converter oscillations under rapidly changing environmental conditions [7],[12],[15],[19]. More advanced techniques based on fuzzy logic, neural networks, and model predictive control have also been investigated; however, they typically require accurate mathematical models, extensive tuning, or relatively powerful embedded hardware, limiting their practical implementation in low-cost standalone PV systems [20]–[24] . Rule-based supervisory control and finite-state implementations have emerged as attractive alternatives because it replaces continuous optimization with deterministic decision rules based on measured operating conditions. By assigning predefined operating states and transition conditions, FSM controllers reduce computational requirements while maintaining reliable converter operation and straightforward implementation on inexpensive embedded platforms [15], [21], [24], [31] .This paper proposes an Experimentally Optimized Priority-Based Finite-State Machine (EO-PFSM) controller for a non-isolated bidirectional buck–boost converter used in a standalone photovoltaic battery charging system. The proposed controller employs experimentally optimized PWM commands together with deterministic state transitions to supervise battery charging while simultaneously incorporating an independent load-management strategy. Unlike many previous studies that rely mainly on simulation or laboratory power supplies, the proposed controller was experimentally validated using a 340 W photovoltaic module charging a 48 V lead–acid battery under real outdoor operating conditions [5], [11], [25]. A total of 1,039 operating samples were recorded during the experimental campaign, of which 1,012 valid steady-state samples were used for statistical evaluation. The proposed system achieved an average experimental conversion efficiency of 94.06%, demonstrating stable charging performance, low computational complexity, and practical suitability for standalone photovoltaic battery charging applications.The remainder of this paper is organized as follows. Section 2 reviews related work and identifies the research gap. Section 3 presents the proposed system architecture and hardware implementation. Section 4 describes the converter design methodology, while Section 5 explains the proposed EO-PFSM charging strategy. Section 6 discusses the experimental results and statistical performance evaluation. Finally, Section 7 concludes the paper and outlines future research directions.

2. Related Work

Standalone photovoltaic battery charging systems have attracted considerable research interest because of their importance in improving energy utilization, extending battery lifetime, and enhancing the reliability of renewable-energy systems [1],[2],[4]. Numerous studies have investigated bidirectional DC–DC converter topologies and charging control strategies to improve power conversion efficiency and charging performance [3],[5],[6].Conventional charging methods generally combine constant-current/constant-voltage (CC–CV) regulation with maximum power point tracking (MPPT) algorithms, including Perturb and Observe (P&O) and Incremental Conductance (INC). These approaches provide satisfactory charging performance under steady operating conditions; however, they rely on continuous duty-cycle adjustment, which may introduce power oscillations and increase computational complexity under rapidly changing environmental conditions [7],[11],[15],[16].To improve dynamic performance, several researchers have proposed intelligent charging techniques based on fuzzy logic, artificial neural networks, model predictive control, and adaptive optimization algorithms [13], [19], [20], [23]. Although these methods generally enhance charging accuracy and dynamic response, they require accurate mathematical models, extensive parameter tuning, or relatively powerful embedded processors, limiting their practical implementation in low-cost standalone photovoltaic systems [21], [22], [24].Finite-state-machine (FSM) control has recently emerged as an attractive alternative because it replaces continuous optimization with deterministic decision rules based on measured operating conditions [15], [21], [24]. By assigning predefined operating states and transition conditions, FSM controllers significantly reduce computational requirements while maintaining reliable converter operation and straightforward implementation on inexpensive embedded platforms .Despite these developments, several limitations remain. Many reported studies focus primarily on converter design or battery charging independently, whereas integrated charging supervision and load management receive comparatively less attention. Furthermore, a considerable proportion of the published work is validated only through simulation or laboratory experiments using regulated DC power supplies rather than actual outdoor photovoltaic conditions [5],[11],[25]. Consequently, the practical performance of simple FSM-based charging strategies under naturally varying solar irradiance remains insufficiently investigated.To address these limitations, this work proposes an Experimentally Optimized Priority-Based Finite-State Machine (EO-PFSM) controller for a non-isolated bidirectional buck–boost converter supplying a 48 V lead–acid battery from a 340 W photovoltaic module. The proposed controller combines deterministic charging-state supervision with an independent load management strategy and is experimentally validated under real outdoor operating conditions. A comparative summary of representative studies and the contribution of the proposed work is presented in Table 1.

Table 1. Comparison of representative battery charging strategies for standalone photovoltaic systems and the proposed EO-PFSM controller.

Ref.	Study	Converter Topology	Control Strategy	Validation	Reported Efficiency	Main Limitation
[5]	Benlahbib *et al.*, 2023	Non-isolated bidirectional Buck–Boost	Dual control for battery charge/discharge	**Experimental**	**96%**	Conventional charge/discharge control without intelligent charging optimization or load management.
[11]	Kurtoğlu and Eroğlu, 2022	Bidirectional DC–DC	Conventional PWM control	Simulation and hardware implementation	**Not Reported**	Focused on converter implementation rather than intelligent battery charging.
[13]	Singh *et al.*, 2024	Non-isolated bidirectional converter	Conventional converter control	Simulation	**Not Reported**	No experimental outdoor validation and no intelligent charging strategy.
[15]	Zhang *et al.*, 2023	Bidirectional DC–DC	Current Observer-Based Critical Conduction Mode	Experimental	**Not Reported**	Increased controller complexity due to observer-based implementation.
[25]	Byun *et al.*, 2025	Four-switch Buck–Boost	Digital PWM control	Experimental	**98.15%**	Designed for multi-cell battery power management rather than standalone PV battery charging.
This Work	Proposed EO-PFSM	Non-isolated bidirectional Buck–Boost	Experimentally Optimized Priority-Based FSM	Outdoor experimental validation	**94.06%**	Low-complexity implementation with integrated load management and experimentally optimized fixed PWM commands.

As summarized in Table 1, previously reported studies primarily focus on converter control, charging algorithms, or converter topologies independently. In contrast, the proposed EO-PFSM controller combines deterministic charging supervision and independent load management within a unified embedded implementation and is experimentally validated under real outdoor photovoltaic conditions. These characteristics distinguish the proposed approach while maintaining a computationally simple control structure and an average conversion efficiency of 94.06%.

3. System Description

3.1 Overall System Configuration

The proposed standalone photovoltaic battery charging system consists of four main subsystems: a 340 W photovoltaic module, a non-isolated bidirectional buck–boost DC–DC converter, a 48 V lead–acid battery bank, and an EO-PFSM supervisory controller. The photovoltaic module serves as the primary energy source, whereas the battery bank stores the harvested energy and supplies the connected DC load whenever the available photovoltaic power becomes insufficient.Figure 1 illustrates the overall architecture of the proposed charging system. During the experimental validation, the converter operated in the boost mode to increase the photovoltaic voltage to the level required for charging the battery. Although the converter hardware inherently supports bidirectional power transfer, this study focuses on experimentally validating the charging operation under real outdoor conditions.The EO-PFSM controller continuously monitors the photovoltaic voltage, photovoltaic current, battery voltage, and battery current to determine the appropriate charging state. In addition, an independent load management algorithm supervises the connected DC load according to predefined battery and photovoltaic voltage thresholds, ensuring that battery charging is always prioritized whenever the available photovoltaic energy becomes insufficient.

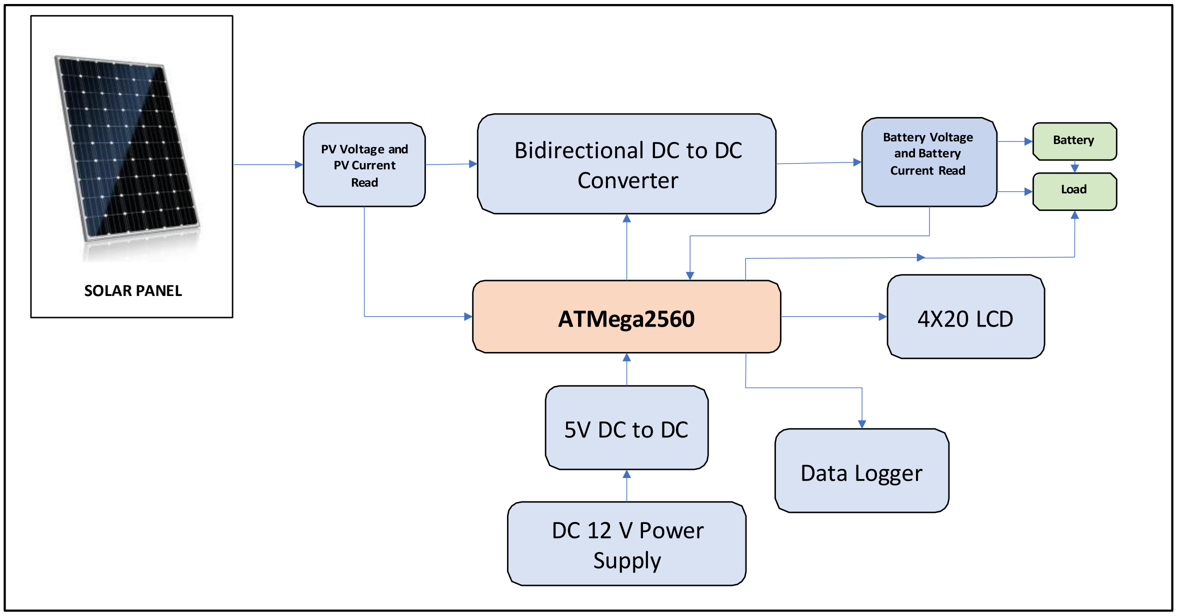

Figure 1. Overall configuration of the proposed standalone photovoltaic battery charging system.

3.2 Experimental Hardware Prototype

The experimental prototype was developed using commercially available components to demonstrate the practical implementation of the proposed controller. The system consists of a 340 W monocrystalline photovoltaic module, a 48 V lead–acid battery bank formed by four 12 V batteries connected in series, and a non-isolated bidirectional buck–boost converter.The converter employs IRFP4668 power MOSFETs driven by an IR2104 half-bridge gate driver operating at a fixed switching frequency of 62.5 kHz[13],[25]. The proposed EO-PFSM controller is implemented using an Arduino Mega 2560, which acquires the measured electrical variables, executes the charging algorithm, and generates the PWM command for the converter.Voltage measurements are obtained using resistive divider circuits, whereas Hall-effect current sensors monitor both the photovoltaic and battery currents[6]. A MicroSD module records all measured electrical variables throughout the outdoor experiment, while a 20 × 4 I²C LCD provides real-time visualization of the operating conditions.

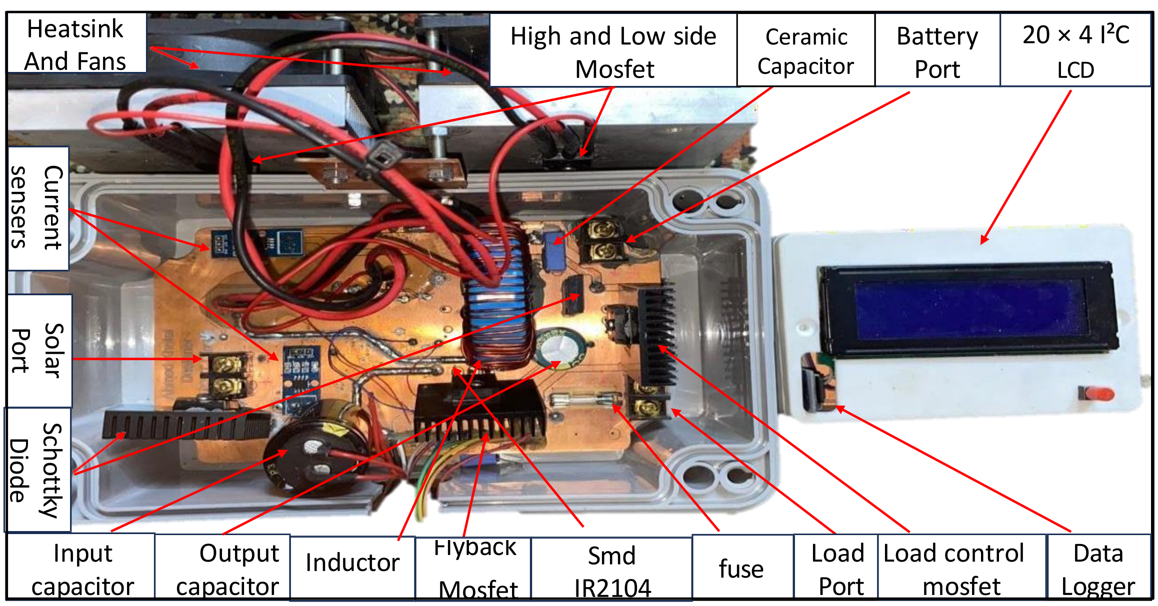

Figure 2. Experimental prototype of the proposed standalone photovoltaic battery charging system.

3.3 Converter Topology

Figure 3 illustrates the proposed non-isolated bidirectional buck–boost converter adopted in this work[2],[13],[28]. The converter employs two power MOSFETs arranged in a synchronous half-bridge configuration, replacing the conventional diode rectifier to reduce conduction losses and improve conversion efficiency[25],[27].During the experimental investigation, the converter operated exclusively in the boost mode to charge the 48 V lead–acid battery from the photovoltaic module. Nevertheless, the developed hardware inherently supports bidirectional power transfer and can be extended to battery discharging applications without structural modifications[3],[28] .A 220 µH inductor together with 330 µF and 220 µF input and output capacitors was selected to reduce current ripple, stabilize the converter voltages, and improve the dynamic response during transitions between charging stages.

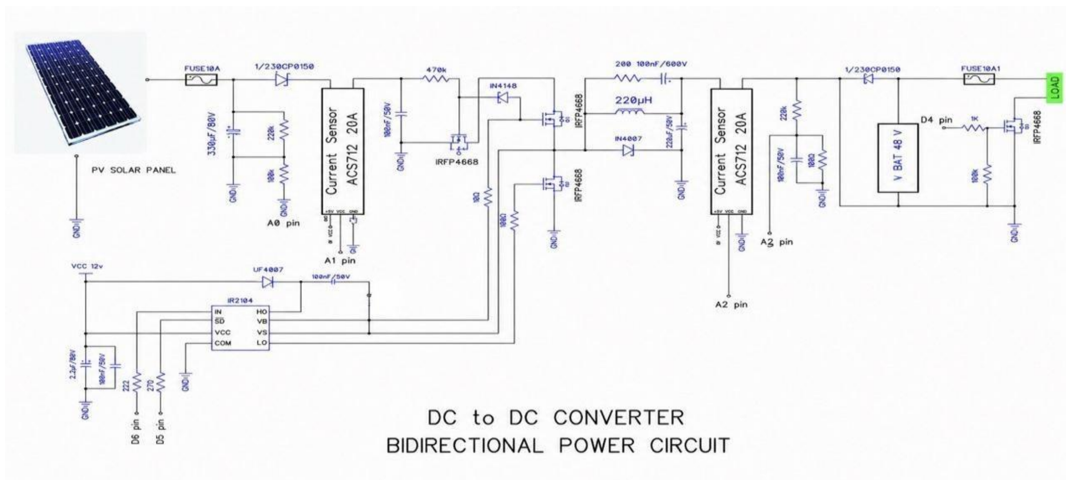

Figure 3. Circuit schematic of the proposed non-isolated bidirectional buck–boost converter.

4. Converter Design

4.1 Design Methodology

The proposed non-isolated bidirectional buck–boost converter was designed to interface a 340 W photovoltaic module with a 48 V lead–acid battery bank. The converter was designed to provide stable charging operation while maintaining high conversion efficiency[6],[27], reduced current ripple, and low implementation complexity suitable for practical embedded applications. A fixed switching frequency of 62.5 kHz was selected as a compromise between switching losses, converter efficiency, passive component size, and microcontroller timing limitations. Experimental evaluation confirmed stable converter operation without excessive semiconductor heating under continuous charging conditions. The passive components were initially determined using conventional converter design equations and subsequently refined through experimental validation[6],[27],[29]. The final hardware employs a 220 µH inductor, a 330 µF input capacitor, and a 220 µF output capacitor, providing stable converter operation, reduced current ripple, and satisfactory voltage regulation throughout the outdoor charging tests. The converter utilizes IRFP4668 power MOSFETs driven by an IR2104 half-bridge gate driver, whereas the EO-PFSM controller is implemented using an Arduino Mega 2560. The principal converter specifications are summarized in Table 2.

Table 2. Design Parameters of the Proposed Bidirectional Buck–Boost Converter

Component	Specification	Function
Photovoltaic Module	Monocrystalline(340 W)	Primary renewable energy source
Open-Circuit Voltage	46.2 V	Maximum PV open-circuit voltage
Voltage at MPP	37.7 V	Maximum power operating voltage

Current at MPP	9.03 A	Maximum power operating current
Battery Bank	4 × 12 V Lead–Acid (Series)	Electrical energy storage
Nominal Battery Voltage	48 V	Battery operating voltage
Battery Capacity	9 Ah	Energy storage capacity
Converter Topology	Non-Isolated Bidirectional Buck–Boost	Power conversion stage
Experimental Operating Mode	Boost Charging	Battery charging mode
Switching Frequency	62.5 kHz	PWM switching frequency
Inductor	220 µH	Current ripple reduction
Input Capacitor	330 µF	PV voltage filtering
Output Capacitor	220 µF	Battery voltage stabilization
Power MOSFET	IRFP4668	Main switching device
Gate Driver	IR2104	MOSFET gate driver
Controller	Arduino Mega 2560	EO-PFSM implementation
Current Sensors	Hall-Effect Sensors	Current measurement
Voltage Sensors	Resistive Divider	Voltage measurement
LCD Display	20 × 4 I²C	Real-time monitoring
Data Logger	MicroSD Module	Experimental data acquisition

Table 2 summarizes the principal electrical and hardware specifications of the developed converter prototype.

4.2 Converter Design Equations

The proposed converter was designed according to the electrical specifications listed in Table 3. The analytical design equations were first employed to estimate the required passive component values, whereas the final component values presented in Table 2 were experimentally refined to obtain stable operation under practical outdoor conditions.

Table 3. Design Specification

Design Parameter	**Symbol**	**Value**
PV Rated Power	(P PV)	340 W
PV Voltage at MPP	(V MPP)	37.7 V
PV Current at MPP	(I MPP)	9.03 A
Battery Nominal Voltage	(V BAT)	48 V
Maximum Charging Voltage	(V MAX)	56.4 V
Battery Capacity	(C BAT)	9 Ah
Switching Frequency	(s)	62.5 kHz
Converter Operating Mode	—	Boost Charging

The voltage conversion ratio of the boost converter [6], [27], [29] is expressed as :

$$\frac{V_{out}}{V_{in}} = \frac{1}{1-D} \qquad (1)$$

from which the required duty cycle is obtained as :

$$D = 1 - \frac{V_{in}}{V_{out}} \qquad (2)$$

The duty-cycle relationship of the proposed bidirectional buck–boost converter is given by (1) [6], [27].

The minimum inductance required to maintain continuous-conduction mode [6], [27], [28] is given by

$$L_{min} = \frac{V_{in}D}{\Delta I_L f_s} \qquad (3)$$

where L is the inductance, ΔIL is the inductor current ripple, and fs is the switching frequency [6], [27], [28].

The corresponding inductor current ripple [27], [29] is:

$$\Delta I_L = \frac{V_{in}D}{Lf_s} \qquad (4)$$

The minimum output capacitance required to satisfy the allowable output voltage ripple [6], [27] is:

$$\boldsymbol{C_{out(min)}} = \frac{I_{out}D}{\Delta V_{out} f_s} \qquad (5)$$

Similarly, the minimum input capacitance is determined [27], [28] from

$$\boldsymbol{C_{in(min)}} = \frac{I_{in}D}{\Delta V_{in} f_s} \qquad (6)$$

Although these analytical expressions were employed during the initial converter design, the final passive component values were experimentally refined according to the measured outdoor charging performance. The selected values provided the best compromise between converter stability, voltage regulation, and current ripple.

4.3 Power Loss Analysis

The efficiency of the proposed converter is mainly influenced by semiconductor conduction losses, switching losses, and passive component losses [27], [29], [30]. The MOSFET conduction loss is expressed as:

$$P_{cond} = I_{RMS}^2 R_{DS(on)} \qquad (7)$$

where $I_{RMS}$is the root-mean-square current and $R_{DS(on)}$is the MOSFET on-state resistance.

The switching loss is approximated by

$$P_{sw} = \frac{1}{2} V_{DS} I_D (t_r + t_f) f_s \qquad (8)$$

where V_{DS}, I_D, t_r, t_f, and $f_s$denote the drain-source voltage, drain current, rise time, fall time, and switching frequency, respectively.

The copper loss of the inductor is calculated as:

$$P_L = I_{L,RMS}^2 R_L \tag{9}$$

The converter input and output powers are obtained experimentally as:

$$P_{in} = V_{PV} I_{PV} \tag{10}$$

$$P_{out} = V_{BAT} I_{BAT} \tag{11}$$

Accordingly, The converter efficiency is calculated using (12) [27], [29]

$$\eta = \frac{P_{out}}{P_{in}} \times 100\% \tag{12}$$

Since the connected DC load was supplied in parallel with the battery bank and its power was not measured independently, the measured battery-side power was adopted as the converter output power throughout the efficiency evaluation.

Instantaneous efficiency values exceeding 100% were occasionally observed because of sensor uncertainty and transient operating conditions. Such values were excluded from the statistical analysis. Based on the **1,012 valid steady-state samples**, the proposed converter achieved an average experimental efficiency of **94.06%**, confirming efficient power conversion under realistic outdoor photovoltaic conditions.

5. Experimentally Optimized Priority-Based Finite-State Machine (EO-PFSM) Charging Strategy

5.1 Controller Overview

The proposed Experimentally Optimized Priority-Based Finite-State Machine (EO-PFSM) controller supervises the charging process of the non-isolated bidirectional buck–boost converter using deterministic decision rules derived from experimental observations [15],[21],[24]. The proposed controller follows a deterministic rule-based supervisory control philosophy, where predefined operating states and experimentally optimized PWM commands are assigned according to the measured operating conditions instead of performing continuous optimization [31]. Unlike conventional charging controllers that continuously optimize the converter duty cycle, the proposed controller directly assigns predefined PWM commands according to the measured operating conditions [21], thereby reducing computational complexity while maintaining reliable battery charging [24],[29] . Figure 4 illustrates the overall control architecture. The controller continuously acquires the photovoltaic voltage, photovoltaic current, battery voltage, and battery current before determining the appropriate charging state. Once the operating state has been identified, the corresponding PWM command is immediately applied to the converter without iterative calculations or continuous duty-cycle perturbation. The proposed controller also incorporates an independent load management algorithm that supervises the connected DC load according to predefined battery and photovoltaic voltage thresholds, ensuring that battery charging remains the primary operating objective. Unlike optimization-based controllers, the proposed EO-PFSM does not continuously compute an optimal duty cycle. Instead, experimentally optimized PWM commands are assigned to predefined operating states.

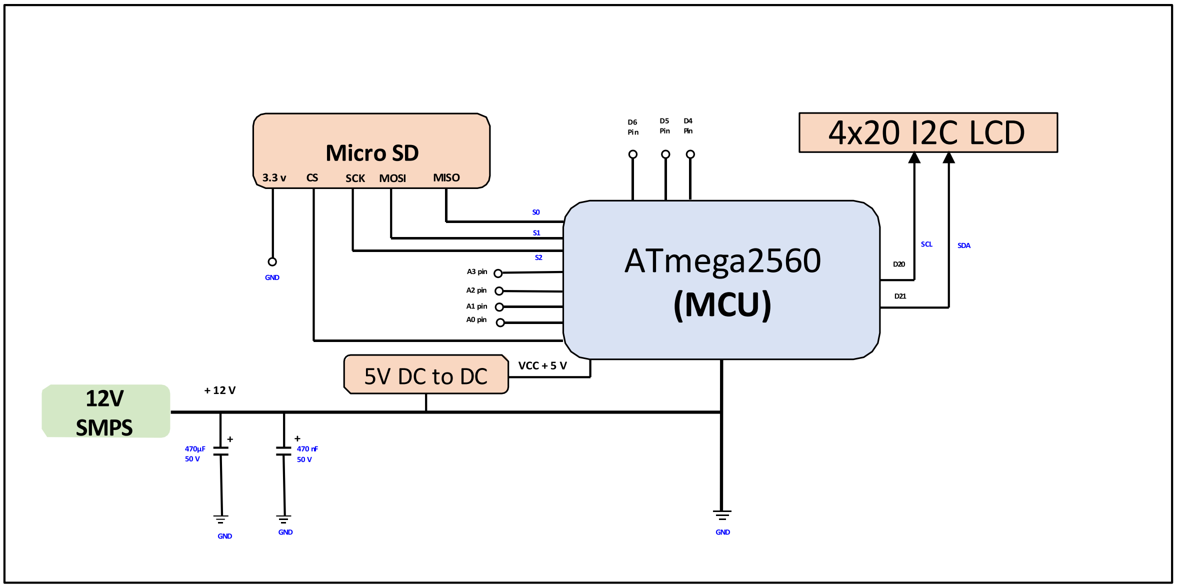

Figure 4. Overall control architecture of the proposed EO-PFSM controller.

5.2 EO-PFSM Operating States

The proposed controller consists of five operating states: OFF, ON, BOOST, BULK, and FLOAT[15],[21]. Each state performs a specific charging function and is associated with an experimentally optimized PWM command.Initially, the controller remains in the OFF state until sufficient photovoltaic voltage is available. After verifying the charging conditions, the controller enters the BOOST state to establish the required voltage gain for battery charging. As the battery voltage increases, the controller automatically transitions to the BULK state, where the highest practical charging power is delivered. Finally, when the battery reaches the recommended charging voltage, the controller switches to the FLOAT state to reduce the charging current while maintaining the battery voltage near its float level. Figure 5 presents the operating-state transition diagram, whereas Table 4 summarizes the operating conditions, PWM commands, and control objectives associated with each charging state.

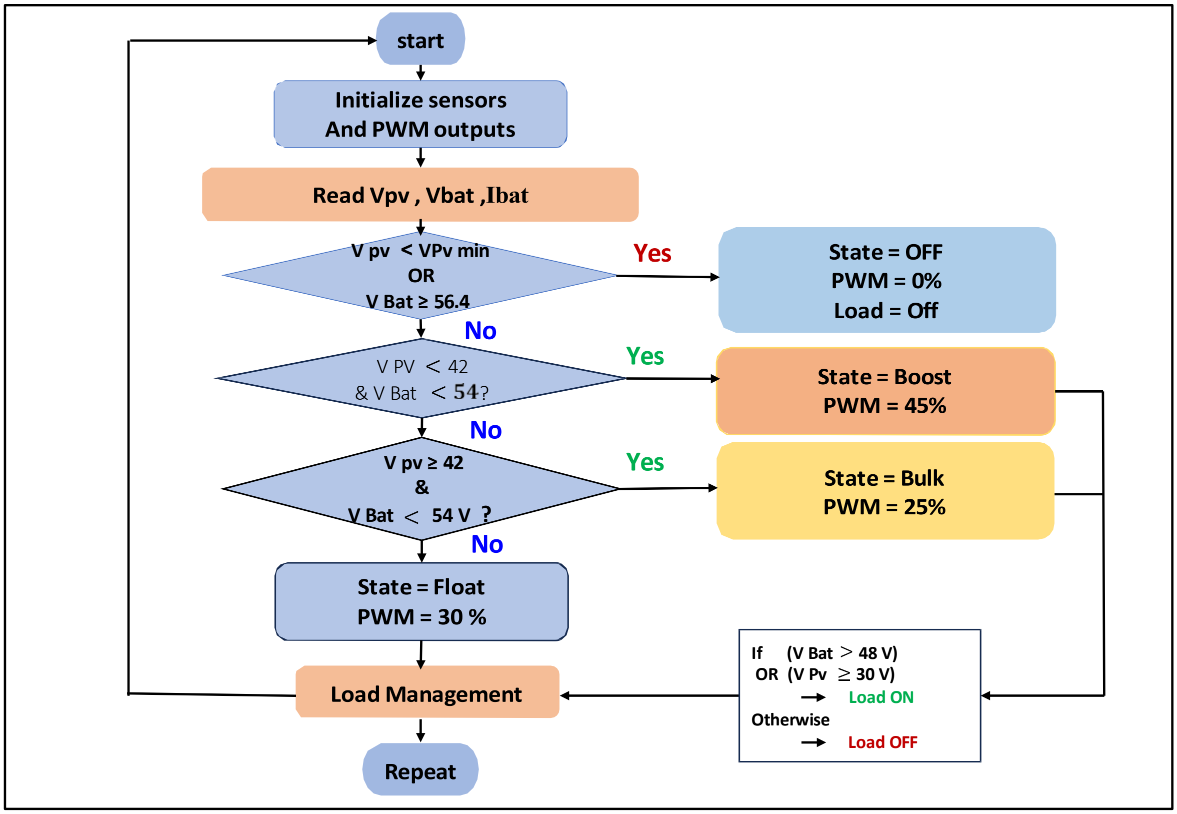

Figure 5. State-transition diagram of the proposed EO-PFSM controller

Table 4. Operating States of the Proposed EO-PFSM Controller

State	Operating Condition	Applied PWM Command (%)	Converter Mode	Control Objective
OFF	(VPV < VPV min) or (VBAT ≥ V MAX)	0	Disabled	Protect the converter and battery under abnormal operating conditions
ON	Initialization completed	Variable	Ready	Prepare the converter for charging operation
BOOST	(V BAT < V BULK)	45	Boost	Establish the required voltage gain for battery charging
BULK	(V BAT<VFLOAT)	25	Boost	Deliver the highest practical charging power
FLOAT	(VBAT ≥VFLOAT)	30	Boost	Maintain the battery near the float voltage while reducing the charging current

Table 4 summarizes the operating states and experimentally optimized PWM commands adopted by the proposed EO-PFSM controller.

5.3 PWM Assignment and Load Management

Instead of continuously adjusting the converter duty cycle, the proposed controller applies experimentally optimized PWM commands for each charging stage. The BOOST, BULK, and FLOAT states employ fixed PWM commands that were experimentally selected to provide stable converter operation and smooth transitions between charging stages under outdoor operating conditions[21],[24].Load management is performed independently of the charging controller [24]. The connected DC load is enabled whenever the battery voltage exceeds 48 V or the photovoltaic voltage exceeds 30 V. Otherwise, the controller disconnects the load to prioritize battery charging and prevent unnecessary battery discharge.The operating-state transition rules and load management conditions are summarized in Tables 5 and 6, respectively.

Table 5. State Transition Rules of the Proposed EO-PFSM Controller

Current State	Transition Condition	Next State	Control Objective
OFF	(V_PV >V PVmin)	BOOST	Enable converter and initiate charging
BOOST	(V BAT < V BULK)	BOOST	Continue initial charging stage
BOOST	(V BAT< V BULK)	BULK	Increase charging power
BULK	(V BAT < V FLOAT)	FLOAT	Enter float charging mode
FLOAT	(V BAT < V FLOAT)	BULK	Resume bulk charging if battery voltage decreases
Any State	(V_PV<VPVmin) or (V_BAT ≥V_MAX)	OFF	Protection and converter shutdown

Table 6. Load Management Decision Rules

Condition	Load Status	Control Objective
(V BAT ≥ 48) V	ON	Battery can safely support the connected load
(V PV ≥ 30) V	ON	Available photovoltaic power can directly supply the load
Otherwise	OFF	Prioritize battery charging and preserve stored energy

The proposed EO-PFSM controller combines deterministic charging supervision with independent load management, enabling stable converter operation while maintaining a simple implementation suitable for low-cost embedded platforms. The experimental validation confirmed reliable transitions between charging stages without unnecessary PWM oscillations or excessive computational requirement .This deterministic implementation is consistent with the low-complexity supervisory control approaches reported for bidirectional DC–DC converters, making the proposed controller suitable for practical embedded applications [31].

6. Experimental Results and Discussion

6.1 Experimental Validation

The proposed EO-PFSM controller was experimentally validated using the hardware prototype described in Section 3. The experimental setup consisted of a 340 W monocrystalline photovoltaic module, a 48 V lead–acid battery bank, and a non-isolated bidirectional buck–boost converter operating at a fixed switching frequency of 62.5 kHz. All electrical quantities were continuously recorded using a MicroSD data logger under naturally varying outdoor photovoltaic conditions.

A total of 1,039 operating samples were collected during approximately two hours of continuous operation. After excluding the startup and transient interval 1,012 valid steady-state samples were retained for the graphical and statistical analyses presented in this section.

6.2 Electrical Performance

Photovoltaic Performance

Figures 6 and 7 present the measured photovoltaic voltage and current during the effective charging interval. Although the photovoltaic current varied continuously because of naturally changing solar irradiance, the photovoltaic voltage remained close to the operating region required for stable converter operation. These observations indicate that the proposed EO-PFSM controller maintained continuous energy extraction from the photovoltaic module without introducing instability into the converter.

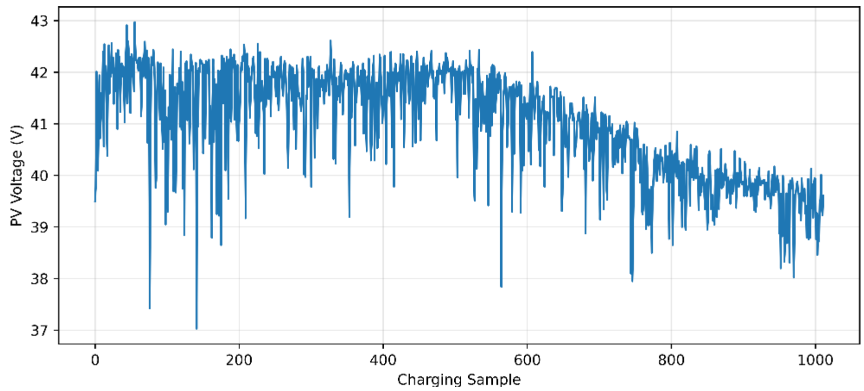

Figure 6. PV Voltage During the Measurement

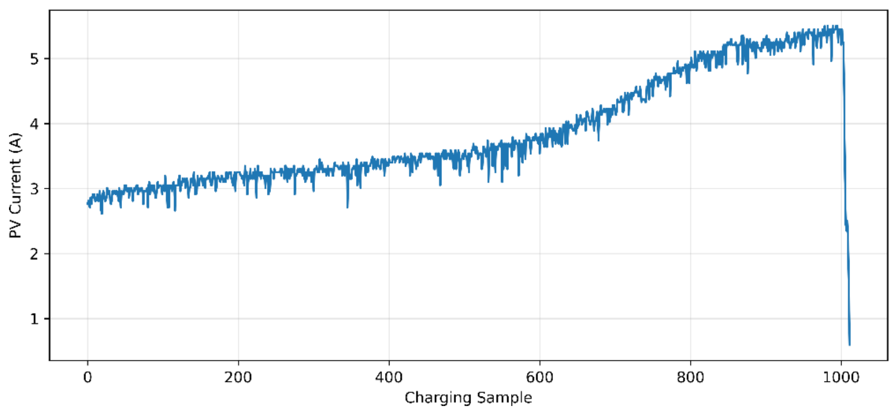

Figure 7. PV Current During the Measurement

Battery Charging Performance

Figures 8 and 9 illustrate the battery voltage and charging current throughout the experiment. The battery voltage increased gradually from approximately 48.4 V to the float charging region above 56 V, confirming the correct implementation of the proposed multi-stage charging strategy. Simultaneously, the charging current decreased progressively as the battery approached full charge, demonstrating the expected transition between the BOOST, BULK, and FLOAT charging stages.

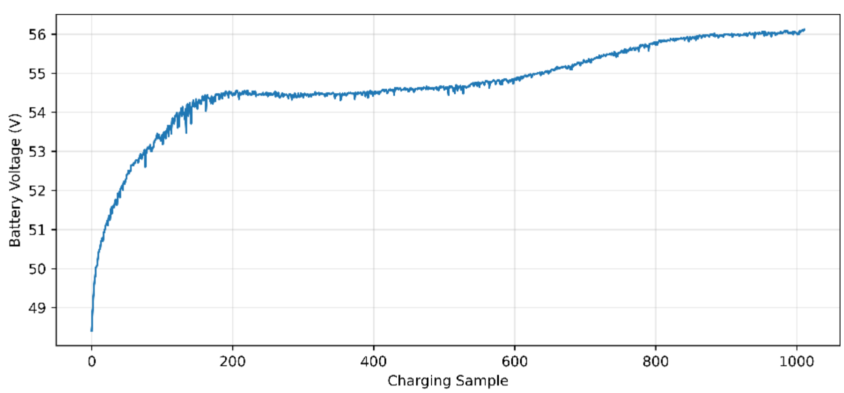

Figure 8. Battery Voltage During Measurement

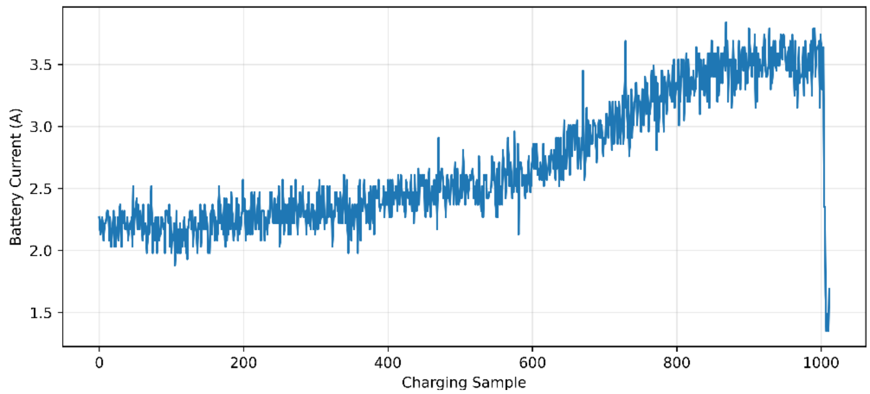

Figure 9. Battery Current During the Measurement

Power Transfer Performance

Figures 10 and 11 show the measured photovoltaic input power and battery charging power. As expected, both quantities varied according to the available solar irradiance. Nevertheless, the proposed controller maintained continuous power transfer throughout the experiment, indicating reliable converter operation under realistic outdoor conditions. The close agreement between the measured input and output powers further confirms the effectiveness of the developed charging system.

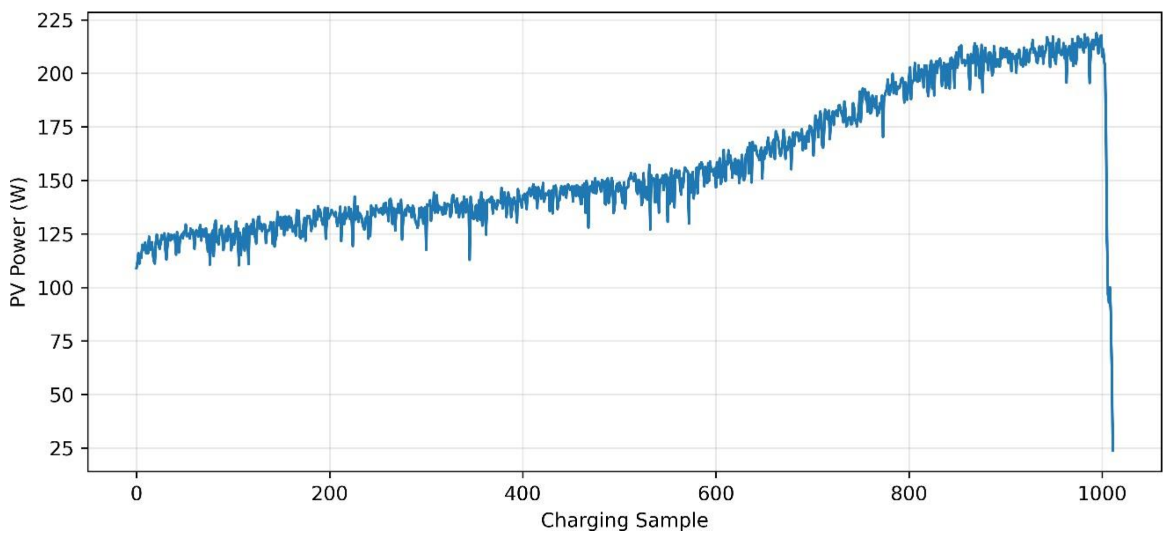

Figure 10. PV Power During the Measurement

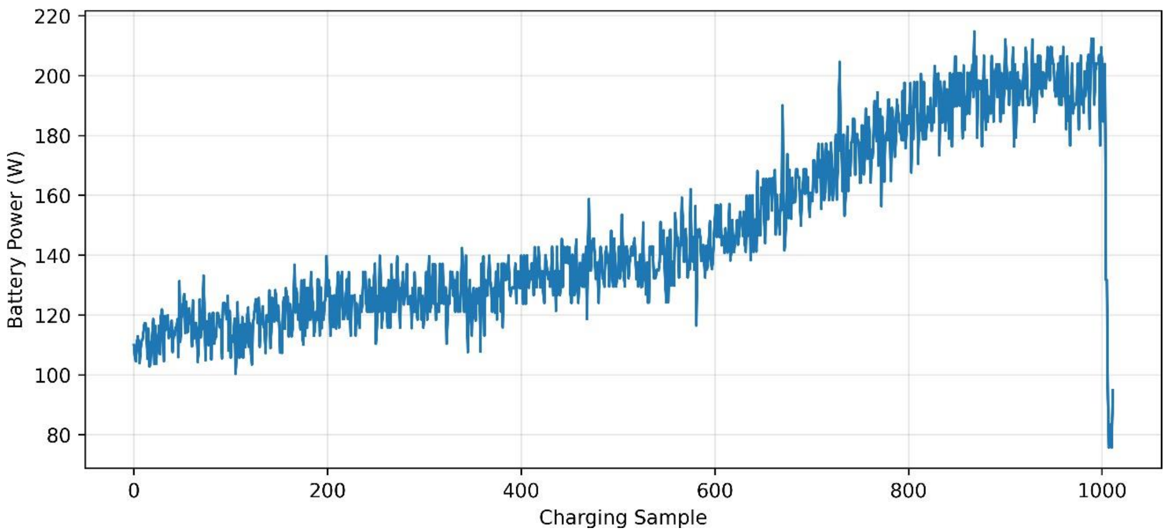

Figure 11. Battery Power During the Measurement

6.3 EO-PFSM Controller Performance

Figure 12 illustrates the operating-state sequence generated by the proposed EO-PFSM controller. The controller performed smooth transitions between the BOOST, BULK, and FLOAT charging stages according to the measured battery voltage without unnecessary oscillations or repeated state changes.

The experimental observations confirm that the proposed EO-PFSM controller successfully coordinated the charging stages while providing predictable converter behavior under naturally varying outdoor operating conditions. Unlike conventional MPPT algorithms, the proposed EO-PFSM maintained constant PWM values inside each charging state, resulting in smooth charging transitions without continuous duty-cycle perturbation.

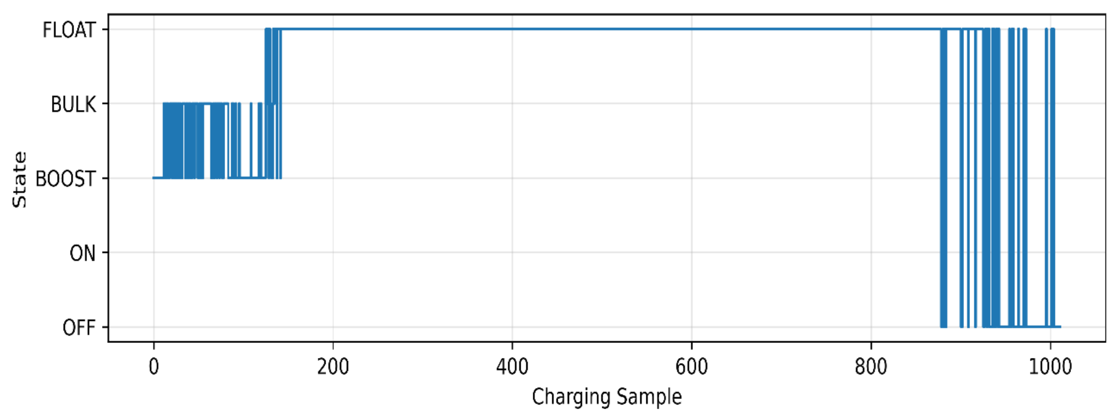

Figure 12. State Sequence

6.4 Statistical Performance Evaluation

The statistical analysis was performed using the 1,012 valid steady-state samples recorded after removing the startup interval. Table 8 summarizes the principal statistical indicators of the measured electrical variables, whereas Table 9 presents the distribution of the EO-PFSM operating states during the experiment.

The statistical results indicate stable converter operation throughout the charging process. The battery voltage increased steadily toward the float charging region, while the charging current gradually decreased according to the charging stage. Furthermore, the operating-state distribution confirms that the controller remained predominantly in the FLOAT state after the battery approached its fully charged condition, demonstrating the effectiveness of the adopted state-transition strategy.

6.5 Converter Efficiency Evaluation

The converter efficiency was calculated using the measured photovoltaic input power and battery-side output power according to

$$\eta = \frac{P_{out}}{P_{in}} \times 100\%$$

where

$$P_{in} = V_{PV} I_{PV}$$

and

$$P_{out} = V_{BAT} I_{BAT}.$$

Because the connected DC load was supplied in parallel with the battery bank and its power was not measured independently, the measured battery-side power was adopted as the converter output power throughout the efficiency evaluation.

After excluding non-physical efficiency values caused by measurement uncertainty during transient operation, the proposed converter achieved an average experimental efficiency of 94.06%, demonstrating effective energy conversion under real outdoor photovoltaic conditions.

6.6 Comparison with Previous Studies

The proposed EO-PFSM controller was compared with representative charging strategies summarized in Table 1. Unlike many previously reported studies that rely mainly on simulation or laboratory power supplies, the present work was experimentally validated using a real photovoltaic module under naturally varying outdoor conditions [5], [11], [25].Furthermore, the proposed controller combines deterministic finite-state control with an independent load management strategy while maintaining low computational complexity suitable for implementation on a low-cost Arduino Mega 2560 platform. The achieved average efficiency of 94.06%, together with stable transitions between the BOOST, BULK, and FLOAT charging stages, demonstrates that the proposed approach provides competitive charging performance without the computational overhead associated with optimization-based charging algorithms.

7. Conclusion

This paper presented the design, implementation, and experimental validation of an Experimentally Optimized Priority-Based Finite-State Machine (EO-PFSM) controller for a non-isolated bidirectional buck–boost DC–DC converter used in a standalone photovoltaic battery charging system. The proposed controller was implemented using an Arduino Mega 2560 and experimentally evaluated with a 340 W photovoltaic module charging a 48 V lead–acid battery under real outdoor operating conditions.Unlike optimization-based charging algorithms that continuously modify the converter duty cycle, the proposed EO-PFSM controller employs deterministic operating states with experimentally optimized PWM commands. This control strategy simplifies the implementation, reduces computational requirements, and provides stable charging performance without iterative optimization.The experimental results demonstrated reliable transitions between the BOOST, BULK, and FLOAT charging stages while maintaining stable converter operation under naturally varying solar irradiance. Statistical analysis performed using 1,012 valid steady-state samples confirmed stable electrical performance and an average experimental converter efficiency of 94.06%. In addition, the independent load management strategy successfully prioritized battery charging while allowing reliable operation of the connected DC load whenever sufficient photovoltaic power or battery energy was available.Overall, the proposed EO-PFSM controller provides an effective balance between charging performance, implementation simplicity, computational efficiency, and practical applicability. The combination of deterministic finite-state control, real outdoor experimental validation, and integrated load management demonstrates the suitability of the proposed approach for standalone photovoltaic battery charging systems.Future work will focus on extending the proposed controller to fully bidirectional energy management, including battery discharging operation and grid-interactive energy storage applications, as well as investigating adaptive supervisory strategies for different battery technologies and operating conditions. The proposed controller can also be extended to lithium-ion battery charging by modifying the state-transition thresholds and charging voltage limits.

References

1. R. M. Babu, M. S. Alam, A. Islam, and M. K. Islam, “Toward Sustainable and Clean Energy Futures: A Techno-Economic Review of Solar PV Systems, Challenges, and Opportunities,” IEEE Access, vol. 13, pp. 169720–169757, 2025, doi: 10.1109/ACCESS.2025.3614771.
2. M. R. Babu et al., “Application of Non-Isolated Bidirectional DC–DC Converters for Renewable and Sustainable Energy Systems: A Review,” Clean Energy, vol. 7, no. 1, 2023, doi: 10.1093/ce/zkac070.
3. Y. Tong, I. Salhi, Q. Wang, G. Lu, and S. Wu, “Bidirectional DC–DC Converter Topologies for Hybrid Energy Storage Systems in Electric Vehicles: A Comprehensive Review,” Energies, vol. 18, no. 9, Art. 2312, 2025, doi: 10.3390/en18092312.
4. M. Faisal, M. A. Hannan, P. J. Ker, A. Hussain, M. B. Mansor, and F. Blaabjerg, “Review of Energy Storage System Technologies in Microgrid Applications: Issues and Challenges,” IEEE Access, vol. 6, pp. 35143–35164, 2018, doi: 10.1109/ACCESS.2018.2841407.
5. B. Benlahbib, A. Dahbi, B. Fares, A. Lakhdari, N. Bouarroudj, S. Mekhilef, and T. Abdelkrim, “An Experimental Investigation Design of a Bidirectional DC–DC Buck–Boost Converter for PV Battery Charger System,” International Journal of Power Electronics and Drive Systems (IJPEDS), vol. 14, no. 4, pp. 2362–2371, 2023, doi: 10.11591/ijpeds.v14.i4.pp2362-2371.
6. M. Kurtoğlu and F. Eroğlu, “Design and Simulation of Bidirectional DC–DC Converter Topology for Battery Applications,” E3S Web of Conferences, vol. 551, Art. 03002, 2024, doi: 10.1051/e3sconf/202455103002.
7. H. Alhusseini, M. Niroomand, and B. Mirzaeian Dehkordi, “A Fuzzy-Based Adaptive P&O MPPT Algorithm for PV Systems With Fast Tracking and Low Oscillations Under Rapidly Irradiance Change Conditions,” IEEE Access, vol. 12, pp. 84374–84386, 2024, doi: 10.1109/ACCESS.2024.3412848.
8. H. Suryoatmojo, I. A. Pratama, and Soedibyo, “Non-Inverting Cascaded Bidirectional Buck–Boost DC–DC Converter with Average Current Mode Control for Lithium-Ion Battery Charger,” Journal on Advanced Research in Electrical Engineering, vol. 5, no. 2, pp. 93–100, 2021.
9. B. Y. Li, C. Xu, C. Li, and Z. Guan, “Working Principle Analysis and Control Algorithm for Bidirectional DC/DC Converter,” Journal of Power Technologies, vol. 97, no. 4, pp. 327–335, 2017.
10. R. Perriment, V. Kumtepeli, M. D. McCulloch, and D. A. Howey, “Lead-Acid Battery Lifetime Extension in Solar Home Systems Under Different Operating Conditions,” in Proc. IEEE PES/IAS PowerAfrica, 2023.
11. M. Kurtoğlu and F. Eroğlu, “Design and Implementation of the Bidirectional DC–DC Converter with Rapid Energy Conversion,” Energies, vol. 15, no. 3, Art. 898, 2022, doi: 10.3390/en15030898.
12. S. Wang et al., “Design and Implementation of an Ultra-High Gain, Soft-Switching, Bidirectional DC–DC Converter with High Efficiency,” e-Prime, vol. 9, Art. 101002, 2025, doi: 10.1016/j.prime.2025.101002.
13. A. K. Singh et al., “A Novel Non-Isolated Bidirectional DC–DC Converter with Improved Current Ripples for Low-Voltage On-Board Charging,” Energies, vol. 17, no. 14, Art. 3570, 2024, doi: 10.3390/en17143570.
14. Recent Developments in Bidirectional DC–DC Converter Topologies, Control Strategies, and Applications in Photovoltaic Power Generation Systems Electronics 2025 DOI:10.3390/electronics14020389
15. Y. Zhang et al., “Current Observer-Based Critical Conduction Mode Control of a Bidirectional DC–DC Converter,” Frontiers in Energy Research, vol. 11, 2023, doi: 10.3389/fenrg.2023.1241718.
16. A. Alshammari et al., “Implementation of an MPPT Technique of a Solar Module with Supervised Machine Learning,” Frontiers in Energy Research, vol. 10, 2022, doi: 10.3389/fenrg.2022.932653.
17. H. Alhusseini et al., “Performance Analysis of a High Gain Bidirectional DC–DC Converter for Renewable Energy Applications,” IEEE Access, 2024, doi: 10.1109/ACCESS.2024.3357726.
18. Design and Control of a Standalone Photovoltaic Power System for Telecommunications in Isolated Regions of Algeria
19. IJEEI 2026 DOI:10.52549/ijeei.v14i1.7679
20. M. Ali et al., “ANFIS-Controlled Boost and Bidirectional Buck–Boost DC–DC Converters,” 2024, doi: 10.1155/2024/6484369.
21. A. El-Shahat et al., “Design of PV, Battery and Supercapacitor-Based Bidirectional DC–DC Converter Using Fuzzy Logic Controller,” 2024, doi: 10.1155/2024/3035524.
22. V. Ny, S. Meas, and C. Srun, “Implementation of Synchronous Bidirectional Converter Using a Fuzzy Logic Controller,” Journal of Electrical and Electronic Engineering, vol. 11, no. 5, pp. 99–114, 2023, doi: 10.11648/j.jeee.20231105.11.
23. E. Martínez-Vera, P. Bañuelos-Sánchez, A. Rosado-Muñoz, J. M. Ramirez-Cortes, and P. Gomez-Gil, “Neuro-Fuzzy Control of a Bidirectional DC–DC Converter Applied in the Powertrain of Electric Vehicles,” Algorithms, vol. 19, no. 5, Art. 335, 2026, doi: 10.3390/a19050335.
24. H. Gaied, A. Flah, H. Kraiem, and C. Z. El-Bayeh, “Three phase bidirectional DC–DC converters based neural network controller for renewable energy sources,” Frontiers in Energy Research, vol. 12, 2024, doi: 10.3389/fenrg.2024.1391310.
25. E. Martínez-Vera and P. Bañuelos-Sánchez, “Review of Bidirectional DC–DC Converters and Trends in Control Techniques for Applications in Electric Vehicles,” IEEE Latin America Transactions, vol. 22, no. 2, pp. 144–155, 2024, doi: 10.1109/TLA.2024.10412031.
26. S.-J. Byun et al., “Design of a High Efficiency Bi-Directional Four-Switch Buck-Boost Converter With HV Gate Driver for Multi-Cell Battery Power Bank Applications,” IEEE Open Journal of Circuits and Systems, vol. 6, pp. 110–119, 2025, doi: 10.1109/OJCAS.2025.3557835.
27. Deep Reinforcement Learning-Based Energy Management for Design and Control of Off-Grid Renewable Microgrids With Dual-Battery Storage DOI:10.1177/01445987251387368

28. S. Aragon-Aviles, A. H. Kadam, T. Sidhu, and S. S. Williamson, “Modeling, Analysis, Design, and Simulation of a Bidirectional DC–DC Converter with Integrated Snow Removal Functionality for Solar PV Electric Vehicle Charger Applications,” Energies, vol. 15, no. 8, Art. 2961, 2022, doi: 10.3390/en15082961.
29. M. A. Alam, A. F. Minai, and F. I. Bakhsh, “Isolated bidirectional DC–DC converter: A topological review,” e-Prime - Advances in Electrical Engineering, Electronics and Energy, vol. 8, Art. 100594, 2024, doi: 10.1016/j.prime.2024.100594.
30. Q. Xu, N. Vafamand, L. Chen, and T. Dragičević, “Review on Advanced Control Technologies for Bidirectional DC/DC Converters in DC Microgrids,” IEEE Journal of Emerging and Selected Topics in Power Electronics, vol. 9, no. 2, pp. 1205–1221, 2021, doi: 10.1109/JESTPE.2020.2978064.
31. X. Li, Y. Liu, and Y. Xue, “Four-Switch Buck–Boost Converter Based on Model Predictive Control With Smooth Mode Transition Capability,” IEEE Transactions on Industrial Electronics, vol. 68, no. 10, pp. 9058–9069, 2021, doi: 10.1109/TIE.2020.3028809.
32. Q. Xu, N. Vafamand, L. Chen, and T. Dragičević, “Review on Advanced Control Technologies for Bidirectional DC/DC Converters in DC Microgrids,” IEEE Journal of Emerging and Selected Topics in Power Electronics, vol. 9, no. 2, pp. 1205–1221, Apr. 2021, doi: 10.1109/JESTPE.2020.2978064.